


Cite this: *RSC Adv.*, 2019, 9, 3900

Exploring unsymmetrical diboranes(4) as boryl ligand precursors: platinum(II) bis-boryl complexes†

 Wiebke Drescher (née Oschmann), Corinna Borner, Daniel J. Tindall
and Christian Kleeberg *

A series of five unsymmetrical platinum(II) bis-boryl complexes, bearing two distinct boryl ligands, are obtained by the oxidative addition reaction of unsymmetrical diborane(4) derivatives, bearing either two different dialkoxy or one dialkoxy and one diamino boryl moiety, with $[(\text{Ph}_3\text{P})_2\text{Pt}(\text{C}_2\text{H}_4)]$. All five complexes were structurally and spectroscopically characterised. The bis-boryl platinum(II) complexes exhibit slightly distorted square-planar *cis*-boryl structures with acute B–Pt–B angles, short B...B distances of 2.44–2.55 Å and relatively long *trans*-boryl P–Pt distances around 2.34 Å. The ^{31}P – ^{195}Pt NMR coupling constants are indicative for the strongly donating/*trans*-influencing boryl ligands. Despite the structural and spectroscopic data at hand no finally conclusive order of the donor properties/*trans*-influence of the boryl ligands can be deduced on the basis of these data. This may be explained by an (residual) interaction of two boryl ligands.

Received 8th January 2019

Accepted 23rd January 2019

DOI: 10.1039/c9ra00170k

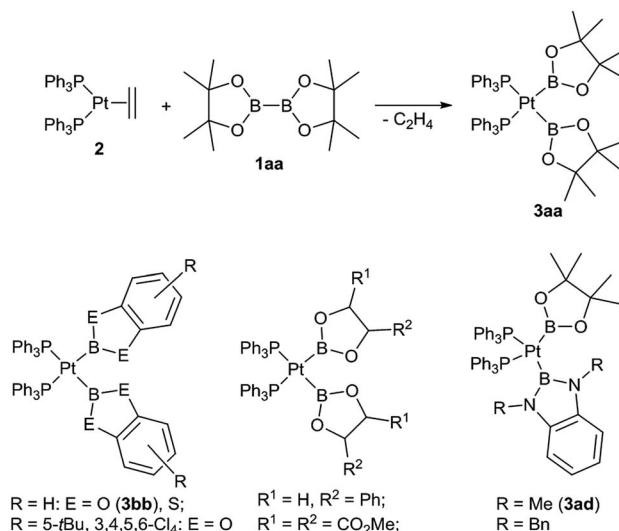
rsc.li/rsc-advances

Introduction

Boryl complexes of transition metals have received considerable attention in the last few years, either due to their role as reactive intermediates in various catalytic processes or due to their unique coordination properties and reactivity of their complexes.^{1,2} In particular a substantial number of boryl platinum(II) complexes have been reported over the last years, amongst these complexes those of the type $(\text{R}_3\text{P})_2\text{Pt}(\text{boryl})_2$ are especially well studied.^{3–6} The latter type of complexes are typically straightforwardly prepared by the oxidative addition reaction of a diborane(4) derivative (1) with a suitable platinum(0) precursor (e.g. $[\text{Pt}(\text{PPh}_3)_2(\text{C}_2\text{H}_4)]$ (2)) and, most importantly, more than 35 complexes of this type are structurally and spectroscopically characterised.^{3–6} About half of these complexes are symmetrical complexes of the specific type $[(\text{Ph}_3\text{P})_2\text{Pt}(\text{boryl})_2]$ (3) with both identical boryl ligands ranging from dialkoxy and diaryloxy boryl ligands but also including ligands such as $\text{BCl}(\text{NMe}_2)$ or BF_2 (Scheme 1). Moreover, we have reported the first unsymmetrical congeners with one dialkoxy and one diamino boryl ligand $[(\text{Ph}_3\text{P})_2\text{Pt}(\text{Bpin})(\text{B}(\text{NR})_2\text{C}_6\text{H}_4)]$ with $\text{R} = \text{Me}$ (3ad) and $\text{R} = \text{Bn}$.³ Hence, complexes of the type

$[(\text{Ph}_3\text{P})_2\text{Pt}(\text{boryl})_2]$ (3) suggest themselves as well suited to comparatively study the coordination properties of different boryl ligands due to their abundant data available and their facile synthesis. In particular, complexes of the type *cis*- $[(\text{Ph}_3\text{P})_2\text{PtXY}]$ (X, Y: anionic ligands) have been especially useful to study the *cis* and the *trans* influence of different anionic ligands X, Y.⁷

We have recently reported the synthesis of a number of unsymmetrical diboranes(4) bearing different dialkoxy as well



Scheme 1 Synthesis of 3aa and examples of complexes $[(\text{Ph}_3\text{P})_2\text{Pt}(\text{boryl})_2]$.^{3,4}

Institut für Anorganische und Analytische Chemie, Technische Universität Carolo-Wilhelmina zu Braunschweig, Hagenring 30, 38106 Braunschweig, Germany.
E-mail: ch.kleeberg@tu-bs.de

† Electronic supplementary information (ESI) available: Additional experimental, NMR spectroscopic and crystallographic data. CCDC 1881532–1881542. For ESI and crystallographic data in CIF or other electronic format see DOI: 10.1039/c9ra00170k



as one dialkoxy and one diaminoboryl moieties (**1**) as potential precursors for boryl complexes.⁸ In this work we endeavour to the study reactivity of these diborane(4) derivatives towards **2** and the coordination properties of the resulting unsymmetrical platinum boryl complexes of the type $[(\text{Ph}_3\text{P})_2\text{Pt}(\text{boryl})(\text{boryl}')]]$. The facile availability of this series of unsymmetrical complexes $[(\text{Ph}_3\text{P})_2\text{Pt}(\text{boryl})(\text{boryl}')]]$ renders a comparative study of sterically and electronically different boryl moieties within one complex fragment for the first time possible.

Experimental

General considerations

The unsymmetrical diboranes(4) **1ab**, **1ac**, **1ae–ag**, **1bd** and **1be** were prepared according to literature procedures.^{3,8} The synthesis and analytical data of **1hh** are described in the ESI.[†] All other compounds were commercially available and were used as received; their purity and identity was checked by appropriate methods. All solvents were dried using MBraun solvent purification systems, deoxygenated using the freeze–pump–thaw method and stored under purified nitrogen. All manipulations were performed using standard Schlenk techniques under an atmosphere of purified nitrogen or in a nitrogen filled glove box (MBraun). NMR spectra were recorded on Bruker Avance II 300, Avance III HD 300, Avance III 500 or Avance 600 spectrometers. For air sensitive samples NMR tubes equipped with screw caps (WILMAD) were used and the solvents were dried over potassium/benzophenone and degassed. Chemical shifts (δ) are given in ppm, using the (residual) resonance signal of the solvents for calibration (C_6D_6 : ^1H NMR: 7.16 ppm, ^{13}C NMR: 128.06 ppm).^{10,11} $\text{B}\{^1\text{H}\}$ and $^{31}\text{P}\{^1\text{H}\}$ NMR chemical shifts are reported relative to external $\text{BF}_3 \cdot \text{Et}_2\text{O}$ and 85% aqueous H_3PO_4 , respectively. $^{13}\text{C}\{^1\text{H}\}$, $^{11}\text{B}\{^1\text{H}\}$ and $^{31}\text{P}\{^1\text{H}\}$ NMR spectra were recorded employing composite pulse ^1H decoupling. If necessary 2D NMR techniques were employed to assign the individual signals (^1H – ^1H NOESY (1 s mixing time), ^1H – ^1H COSY, ^1H – ^{13}C HSQC, ^1H – ^{13}C HMBC and ^1H – ^{31}P HMBC). Melting points were determined in flame sealed capillaries under nitrogen using a Büchi 535 apparatus and are not corrected. Elemental analyses were performed at the Institut für Anorganische und Analytische Chemie of the Technische Universität Carolo-Wilhelmina zu Braunschweig using an Elementar vario MICRO cube instrument. GC/MS measurements were performed using a Shimadzu GCMS-QP2010SE instrument operating in positive EI mode (70 eV, 60–700 m/z) with the following conditions: injection temperature 250 °C; interface temperature 280 °C; temperature program: start temperature 50 °C for 3 min, heating rate 12 °C min^{-1} , end temperature 300 °C for 8 min or 38 min; column type: ZB-5MS GUARDIAN, 30 m \times 0.25 mm, 0.25 μm film thickness; He carrier gas (1.5 mL min^{-1}). High resolution GC/MS measurements were performed by the Analytical Facility at the Technische Universität Carolo-Wilhelmina zu Braunschweig using an Agilent 6890 GC instrument coupled to a Accu-TOF GC JMS-T100GC (JOEL) mass spectrometer operating in positive EI mode (70 eV) with the following conditions: injection temperature 250 °C; interface temperature 270 °C; temperature

program: start temperature 50 °C for 3 min, heating rate 10 °C min^{-1} , end temperature 310 °C for 3 min; column type: ZB-5MS, 30 m \times 0.25 mm, 0.25 μm film thickness; He carrier gas (1.0 mL min^{-1}).

X-ray diffraction studies. The crystals were, inside a nitrogen-filled glovebox, transferred into inert perfluoroether oil and, outside of the glovebox, rapidly mounted on top of a human hair or a MITEGEN mount and placed in the cold nitrogen gas stream on the diffractometer.^{11a} The data were either collected on an Oxford Diffraction Xcalibur Eos instrument using graphite monochromated MoK_α radiation (conventional sealed X-ray tube), an Oxford Diffraction Nova Atlas instrument using mirror-focused CuK_α radiation (micro focus source) or an Rigaku Oxford Diffraction XtaLAB Synergy HyPix instrument using mirror-focused MoK_α radiation (micro focus source). The reflections were indexed, integrated and absorption corrections applied as implemented in the CrysAlisPro software.^{9,11b} The structures were solved employing the programs SHELXT or SHELXS and refined anisotropically for all non-hydrogen atoms by full-matrix least squares on all F^2 using SHELXL software.^{11c–e} Generally hydrogen atoms were refined employing a riding model; methyl groups were treated as rigid bodies and were allowed to rotate about the E– CH_3 bond. During refinement and analysis of the crystallographic data the programs WinGX, PLATON, DSR, Mercury and Diamond were used.^{11f,j} Unless noted otherwise the shown ellipsoids represent the 50% probability level and the hydrogen atoms are omitted for clarity; adapted numbering schemes may be used to facilitate readability.

[Pt(PPh₃)₂(Bpin)(Bcat)] (3ab). $[\text{Pt}(\text{PPh}_3)_2(\text{C}_2\text{H}_4)]$ (**2**) (50 mg, 67 μmol , 1.0 eq.) and pinB–Bcat (**1ab**) (16.4 mg, 67 μmol , 1.0 eq.) were mixed in toluene (5 mL). The red solution was stirred at room temperature for 5 h whilst flask was evacuated for a few seconds every 60 min. The solvent was removed under reduced pressure to give a brownish solid, from which after recrystallization by vapour diffusion of *n*-pentane in a benzene solution at room temperature colourless (single) crystals of **3ab**(C_6H_6)_{1/2} (39 mg, 39 μmol , 58%) were obtained after drying *in vacuo*. Mp 189 °C (decomposition, from *n*-pentane/ C_6H_6). Found: C, 60.95; H, 5.2. Calc. for $\text{C}_{54}\text{H}_{52}\text{B}_2\text{O}_4\text{P}_2\text{Pt}$ (**3ab**(C_6H_6)_{1/2}): C, 61.0; H, 4.9 (composition in agreement with NMR data, the composition found in the single crystal structure determination is **3ab**(C_6H_6)). δ_{H} (500 MHz, C_6D_6 , rt): 0.78 (12H, s, $\text{OC}(\text{CH}_3)_2$), 6.71 (2H, virt. dd, $J = 3.4, 5.8$ Hz, CH_{cat}), 6.73–6.83 (9H, m, $\text{CH}_{\text{PPh}_3}(\text{trans-Bpin})$), 6.91–6.94 (9H, m, $\text{CH}_{\text{PPh}_3}(\text{trans-Bcat})$), 6.94 (2H, virt. dd, $J = 3.4, 5.8$ Hz, CH_{cat} (overlapping with previous signal)), 7.48–7.54 (6H, m, 2- $\text{CH}_{\text{PPh}_3}(\text{trans-Bpin})$), 7.58–7.65 (6H, m, 2- $\text{CH}_{\text{PPh}_3}(\text{trans-Bcat})$). $\delta_{^{13}\text{C}\{^1\text{H}\}}$ (125 MHz, C_6D_6 , rt): 25.1 ($\text{OC}(\text{CH}_3)_2$), 81.7 (d, $J_{\text{C-P}} = 3.0$ Hz, $J_{\text{C-Pt}} = 34$ Hz (satellites), $\text{OC}(\text{CH}_3)_2$), 111.0 (CH_{cat}), 120.3 (CH_{cat}), 127.8 (d, $J_{\text{C-P}} = 2.2$ Hz, 3- $\text{CH}_{\text{PPh}_3}(\text{trans-Bcat})$), 127.9 (d, $J_{\text{C-P}} = 2.5$ Hz, 3- $\text{CH}_{\text{PPh}_3}(\text{trans-Bpin})$), 129.4 (d, $J_{\text{C-P}} = 1.5$ Hz, 4- $\text{CH}_{\text{PPh}_3}(\text{trans-Bpin})$), 129.5 (d, $J_{\text{C-P}} = 1.5$ Hz, 4- $\text{CH}_{\text{PPh}_3}(\text{trans-Bcat})$), 134.3 (d, $J_{\text{C-P}} = 13.6$ Hz, $J_{\text{C-Pt}} = 13$ Hz (satellites), 2- $\text{CH}_{\text{PPh}_3}(\text{trans-Bpin})$), 135.2 (d, $J_{\text{C-P}} = 12.5$ Hz, $J_{\text{C-Pt}} = 14$ Hz (satellites), 2- $\text{CH}_{\text{PPh}_3}(\text{trans-Bcat})$), 136.2 (dd, $J_{\text{C-P}} = 39, 3$ Hz, 1- $\text{C}_{\text{PPh}_3}(\text{trans-Bpin})$), 136.3 (d, $J_{\text{C-P}} = 39, 4$ Hz, 1- $\text{C}_{\text{PPh}_3}(\text{trans-Bcat})$), 151.2 (d, $J_{\text{C-P}} = 2.6$ Hz, C_{cat}). $\delta_{^{31}\text{P}\{^1\text{H}\}}$



(202 MHz, C₆D₆, rt): 28.7 (*J*_{P-Pt} = 1690 Hz (satellites), P_{PPh₃}(*trans*-Bcat)), 35.5 (*J*_{P-Pt} = 1565 Hz (satellites), P_{PPh₃}(*trans*-Bpin)). A ¹¹B {¹H} NMR signal could not be detected.

[Pt(PPh₃)₂(Bpin)(Bneop)] (3ac). [Pt(PPh₃)₂(C₂H₄)] (2) (50 mg, 67 μmol, 1.0 eq.) and pinB-Bneop (**1ac**) (16.0 mg, 67 μmol, 1.0 eq.) were mixed in toluene (5 mL). The orange-red solution was stirred at room temperature for 3 h whilst flask was evacuated for a few seconds every 30 min. The solvent was removed under reduced pressure to give an orange-red solid. The latter was recrystallised by vapour diffusion of *n*-pentane into a THF solution at room temperature. The product was obtained as a colourless single crystalline solid (21 mg, 22 μmol, 33%). The mother liquor was layered with additional *n*-pentane to give additional slightly less pure product as a pale orange solid (12 mg, 13 μmol, 19%). Mp 149 °C (decomposition, from *n*-pentane/THF). Found: C, 59.05; H, 5.4%. Calc. for C₄₇H₅₂B₂-O₄P₂Pt (**3ac**): C, 58.8; H, 5.5%. δ_H (500 MHz, C₆D₆, rt): 0.79 (6H, s, (O(CH₂))₂C(CH₃)₂), 1.04 (12H, s, OC(CH₃)₂), 3.04 (4H, s, (O(CH₂))₂C(CH₃)₂), 6.86–6.96 (18H, m, CH_{PPh₃}), 7.57–7.66 (6H, m, 2-CH_{PPh₃}(*trans*-Bneop)), 7.64–7.70 (6H, m, 2-CH_{PPh₃}(*trans*-Bpin)). δ¹³C{¹H} (125 MHz, C₆D₆, rt): 23.1 (OC(CH₃)₂), 25.6 ((O(CH₂))₂C(CH₃)₂), 31.9 ((O(CH₂))₂C(CH₃)₂), 72.0 (d, *J*_{C-P} = 4 Hz, *J*_{C-Pt} = 44 Hz (satellites) (O(CH₂))₂C(CH₃)₂), 80.9 (d, *J*_{C-P} = 3 Hz, *J*_{C-Pt} = 38 Hz (satellites), OC(CH₃)₂), 127.7 (d, *J*_{C-P} = 10 Hz, 3-CH_{PPh₃}), 127.9 (d, *J*_{C-P} = 10 Hz, 3-CH_{PPh₃}), 129.0 (br. d, *J*_{C-P} = 1.2 Hz, 4-CH_{PPh₃}), 129.1 (br. s, 4-CH_{PPh₃}), 134.7 (d, *J*_{C-P} = 13 Hz, *J*_{C-Pt} = 13 Hz (satellites), 2-CH_{PPh₃}(*trans*-Bpin)), 135.1 (d, *J*_{C-P} = 13 Hz, *J*_{C-Pt} = 13 Hz (satellites), 2-CH_{PPh₃}(*trans*-Bneop)), 137.0–137.8 (m, 1-C_{PPh₃}). δ³¹P{¹H} (202 MHz, C₆D₆, rt): 27.5 (*J*_{P-Pt} = 1455 Hz (satellites), P_{PPh₃}(*trans*-Bneop)), 33.7 (*J*_{P-Pt} = 1585 Hz (satellites), P_{PPh₃}(*trans*-Bpin)). δ¹¹B{¹H} (161 MHz, C₆D₆, rt): 51 (br. s, Δ*w*_{1/2} = 2500 Hz).

[Pt(PPh₃)₂(Bpin)(BMeEn)] (3ae). [Pt(PPh₃)₂(C₂H₄)] (2) (50 mg, 67 μmol, 1.0 eq.) and pinB-BMeEn (**1ae**) (14.4 mg, 67 μmol, 1.0 eq.) were mixed in toluene (5 mL). The orange-red solution was stirred at room temperature for 3 h whilst flask was evacuated for a few seconds every 30 min. The solvent was removed under reduced pressure. The orange-red solid was recrystallised by vapour diffusion of *n*-pentane into a THF solution at room temperature to give analytically pure (**3ae**(thf)_{1.5}) (48 mg, 46 μmol, 68%) as colourless crystalline solid (suitable for X-ray diffraction analysis). Mp 160 °C (decomposition, from *n*-pentane/THF). Found: C, 59.4; H, 6.4; N, 3.1%. Calc. for C₅₂-H₆₄B₂N₂O_{3.5}P₂Pt (**3ae**(thf)_{1.5}): C, 59.4; H, 6.1; N, 2.7% (composition in agreement with NMR data and single crystal structure analysis (Table 1). δ_H (500 MHz, C₆D₆, rt): 0.99 (12H, s, OC(CH₃)₂), 2.67–2.72 (2H, m, NCH₂), 2.95 (6H, s, NCH₃), 3.07–3.12 (2H, m, NCH₂), 6.88–6.94 (9H, m, CH_{PPh₃}(*trans*-Bpin)), 6.94–7.01 (9H, m, CH_{PPh₃}(*trans*-BMeEn)), 7.53–7.60 (6H, m, 2-CH_{PPh₃}(*trans*-Bpin)), 7.62–7.68 (6H, m, 2-CH_{PPh₃}(*trans*-BMeEn)). δ¹³C{¹H} (125 MHz, C₆D₆, rt): 25.3 (OC(CH₃)₂), 37.1 (s, *J*_{C-Pt} = 32 Hz (satellites), NCH₃), 53.7 (d, *J*_{C-P} = 4.5 Hz, *J*_{C-Pt} = 42 Hz (satellites), NCH₂), 80.9 (d, *J*_{C-P} = 3.0 Hz, *J*_{C-Pt} = 36 Hz (satellites), OC(CH₃)₂), 127.5 (d, *J*_{C-P} = 9.4 Hz, 3-CH_{PPh₃}(*trans*-Bpin)), 127.8 (d, *J*_{C-P} = 8.9 Hz, 3-CH_{PPh₃}(*trans*-BMeEn)), 129.1 (d, *J*_{C-P} = 1.4 Hz, 4-CH_{PPh₃}(*trans*-BMeEn)), 129.2 (d, *J*_{C-P} = 1.3 Hz, 4-CH_{PPh₃}(*trans*-Bpin)), 134.8 (d, *J*_{C-P} = 13.9 Hz, *J*_{C-Pt} = 14 Hz

(satellites), 2-CH_{PPh₃}(*trans*-Bpin)), 135.1 (d, *J*_{C-P} = 13.0 Hz, *J*_{C-Pt} = 13 Hz (satellites), 2-CH_{PPh₃}(*trans*-BMeEn)), 137.3 (dd, *J*_{C-P} = 33, 4 Hz, 1-C_{PPh₃}(*trans*-Bpin)), 137.6 (dd, *J*_{C-P} = 32, 4 Hz, 1-C_{PPh₃}(*trans*-BMeEn)). δ³¹P{¹H} (202 MHz, C₆D₆, rt): 31.1 (*J*_{P-Pt} = 1590 Hz (satellites), P_{PPh₃}(*trans*-BMeEn)), 36.1 (*J*_{P-Pt} = 1615 Hz (satellites), P_{PPh₃}(*trans*-Bpin)). δ¹¹B{¹H} (161 MHz, C₆D₆, rt): 47 (br. s, Δ*w*_{1/2} = 1600 Hz).

[Pt(PPh₃)₂(Bcat)(Bdmab)] (3bd). [Pt(PPh₃)₂(C₂H₄)] (2) (50 mg, 67 μmol, 1.0 eq.) and catB-Bdmab (**1bd**) (17.6 mg, 67 μmol, 1.0 eq.) were mixed in toluene (3 mL). The red solution was stirred at room temperature for 3 h whilst flask was evacuated for a few seconds every 30 min. The solvent was removed under reduced pressure to give a brownish-red solid (38 mg, 38 μmol, 58%). Single crystals suitable for X-ray diffraction analysis were obtained by vapour diffusion of *n*-pentane into a benzene solution at room temperature. Mp 165 °C (decomposition). Found: C, 60.9; H, 4.7; N, 2.4%. Calc. for C₅₀H₄₄B₂N₂O₂P₂Pt (**3bd**): C, 61.1; H, 4.5; N, 2.6%. δ_H (500 MHz, C₆D₆, rt): 3.33 (6H, s, NCH₃), 6.55 (2H, virt. dd, *J* = 3.3, 5.7 Hz, CH_{cat}), 6.61 (2H, virt. dd, *J* = 3.2, 5.7 Hz, 2-CH_{dmab}), 6.71–6.75 (6H, m, 3-CH_{PPh₃}(I)), 6.81–6.86 (2 + 3H, m, CH_{cat}+4-CH_{PPh₃}(I)), 6.86–6.92 (9H, m, 3+4-CH_{PPh₃}(II)), 6.94 (2H, virt. dd, *J* = 3.2, 5.7 Hz, 3-CH_{dmab}), 7.34–7.40 (6H, m, 2-CH_{PPh₃}(I)), 7.58–7.64 (6H, m, 2-CH_{PPh₃}(II)). δ¹³C{¹H} (125 MHz, C₆D₆, rt): 39.9 (s, NCH₃), 106.3 (2-CH_{dmab}), 111.1 (3-CH_{cat}), 116.9 (3-CH_{dmab}), 120.4 (2-CH_{cat}), 127.7 (d, *J*_{C-P} = 9.2 Hz, 3-CH_{PPh₃}(I)), 128.1 (d, *J*_{C-P} = 9.4 Hz, 3-CH_{PPh₃}(II)), 129.5 (d, *J*_{C-P} = 1.6 Hz, 4-CH_{PPh₃}(II)), 129.6 (d, *J*_{C-P} = 1.4 Hz, 4-CH_{PPh₃}(I)), 134.1–134.5 (m, 2-CH_{PPh₃}(I + II)), 135.8 (dd, *J*_{C-P} = 39, 3 Hz, m, 2-C_{PPh₃}(I)), 136.2 (dd, *J*_{C-P} = 38, 3 Hz, m, 2-C_{PPh₃}(II)), 141.6 (d, *J*_{C-P} = 3.1 Hz, m, 1-C_{dmab}), 150.7 (d, *J*_{C-P} = 2.8 Hz, m, 1-C_{cat}). δ³¹P{¹H} (202 MHz, C₆D₆, rt): 31.0 (*J*_{P-Pt} = 1650 Hz (satellites), P_{PPh₃}(II)), 33.7 (*J*_{P-Pt} = 1715 Hz (satellites), P_{PPh₃}(I)). A ¹¹B{¹H} NMR signal could not be detected.

[Pt(PPh₃)₂(Bcat)(BMeEn)] (3be). [Pt(PPh₃)₂(C₂H₄)] (2) (50 mg, 67 μmol, 1.0 eq.) and catB-BMeEn (**1be**) (14.4 mg, 67 μmol, 1.0 eq.) were mixed in toluene (3 mL). The red solution was stirred at room temperature for 3 h whilst flask was evacuated for a few seconds every 30 min. The solvent was removed under reduced pressure to give a brownish-red solid (42 mg, 45 μmol, 67%). Single crystals of the benzene solvate of **3be** suitable for X-ray diffraction analysis were obtained by vapour diffusion of *n*-pentane into a benzene solution at room temperature. **3be**(C₄H₈O)_{1/2} was obtained by recrystallization from *n*-pentane/THF at –40 °C as microcrystalline powder. Mp 121 °C (decomposition, from *n*-pentane/THF). Found: C, 59.4; H, 5.3; N, 3.3%. Calc. for C₅₀H₅₂B₂N₂O₃P₂Pt (**3be**(C₄H₈O)_{1/2}): C, 59.3; H, 5.0; N, 2.9% (composition in agreement with NMR data). δ_H (500 MHz, C₆D₆, rt): 2.47–2.53 (2H, br t, *J* = 7.7 Hz, NCH₂), 2.85–2.90 (2H, br t, *J* = 7.7 Hz, NCH₂), 2.99 (6H, s, NCH₃), 6.65 (2H, virt. dd, *J* = 3.3, 5.7 Hz, CH_{cat}), 6.83–6.94 (18H, m, CH_{PPh₃}), 7.00 (2H, virt. dd, *J* = 3.3, 5.7 Hz, CH_{cat}), 7.54–7.64 (m, 12H, CH_{PPh₃}). δ¹³C{¹H} (125 MHz, C₆D₆, rt): 36.9 (s, *J*_{C-Pt} = 30.3 Hz (satellites), NCH₃), 53.3 (d, *J*_{C-P} = 4.4 Hz, *J*_{C-Pt} = 41 Hz (satellites), NCH₂), 111.0 (CH_{cat}), 120.3 (CH_{cat}), 127.4 (d, *J*_{C-P} = 9.6 Hz, CH_{PPh₃}), 127.7 (d, *J*_{C-P} = 9.2 Hz, CH_{PPh₃}), 128.9 (d, *J*_{C-P} = 1.6 Hz, CH_{PPh₃}), 129.2 (d, *J*_{C-P} = 1.5 Hz, CH_{PPh₃}), 134.4 (d, *J*_{C-P} = 12.7 Hz, *J*_{C-Pt} = 14 Hz (satellites), CH_{PPh₃}), 134.8 (d, *J*_{C-P} =





Table 1 Crystallographic data collection parameter of **3ab**(C₆H₆), **3ac**, **3ae**(C₄H₈O)_{1.5}, **3bd**, **3be**(C₆H₆), **3cc**(C₄H₈O) and **3hh**(C₄H₈O)

Compound	3ab (C ₆ H ₆)	3ac	3ae (C ₄ H ₈ O) _{1.5} ^b	3bd	3be (C ₆ H ₆)	3cc (C ₄ H ₈ O) ^c	3hh (C ₄ H ₈ O)
Formula	C ₃₄ H ₃₂ B ₂ O ₄ P ₂ Pt	C ₁₇ H ₁₂ B ₂ O ₄ P ₂ Pt	C ₅₂ H ₆₄ B ₂ O _{3.5} P ₂ Pt	C ₅₀ H ₄₄ B ₂ N ₂ O ₂ P ₂ Pt	C ₅₂ H ₅₀ B ₂ N ₂ O ₂ P ₂ Pt	C ₅₀ H ₅₈ B ₂ O ₃ P ₂ Pt	C ₅ H ₁₂ B ₂ N ₂ O ₃ P ₂ Pt
<i>M_r</i> /(g mol ⁻¹)	1043.60	959.53	1051.70	983.52	1013.59	1017.61	1055.62
Crystal shape	Rod	Irregular block	Rhombohedral	Block	Prism	Fragment of rod	Fragment of block
Crystal colour	Clear colourless	Clear colourless	Clear colourless	Clear pale yellow	Clear light orange	Clear colourless	Clear light yellow
Cryst. dim./mm ³	0.49 × 0.13 × 0.06	0.40 × 0.33 × 0.21	0.32 × 0.17 × 0.16	0.55 × 0.36 × 0.28	0.53 × 0.25 × 0.25	0.41 × 0.23 × 0.11	0.41 × 0.26 × 0.22
Crystal system	Triclinic	Orthorhombic	Monoclinic	Triclinic	Triclinic	Triclinic	Monoclinic
Space group (no.)	<i>P</i> 1 (2)	<i>Pbca</i> (61)	<i>P</i> 2 ₁ / <i>c</i> (14)	<i>P</i> 1 (2)	<i>P</i> 1 (2)	<i>P</i> 1 (2)	<i>P</i> 2 ₁ / <i>c</i> (14)
<i>a</i> /Å	13.1742(5)	18.1455(3)	13.1260(3)	13.4322(3)	9.9026(5)	12.6111(6)	22.1926(3)
<i>b</i> /Å	15.3010(5)	14.2463(3)	12.8989(3)	13.6477(4)	11.8550(5)	14.3974(7)	10.4677(2)
<i>c</i> /Å	24.3714(13)	33.2215(7)	29.1381(6)	14.5369(4)	21.5121(9)	14.9326(7)	20.6740(3)
α	73.469(4)°	90°	90°	70.017(2)°	94.470(3)°	68.803(5)°	90°
β	89.111(4)°	90°	100.612(2)°	82.459(2)°	96.674(4)°	66.072(5)°	105.849(2)°
γ	87.082(3)°	90°	90°	60.926(3)°	114.620(4)°	88.190(4)°	90°
<i>V</i> /Å ³	4703.6(4)	8588.0(3)	4849.0(2)	2186.9(1)	2257.8(2)	2289.4(2)	4620.1(1)
<i>Z</i> , <i>Z'</i>	4, 2	8, 1	4, 2	2, 1	2, 1	2, 1	4, 1
<i>D</i> _{calcd.} /(g cm ⁻³)	1.474	1.484	1.441	1.494	1.491	1.476	1.518
μ /mm ⁻¹ (λ/Å)	3.097 (0.71073)	3.384 (0.71073)	3.005 (0.71073)	3.319 (0.71073)	3.221 (0.71073)	3.180 (0.71073)	3.153 (0.71073)
Absorption corr.	Analytical	Gaussian	Gaussian	Analytical	Analytical	Gaussian	Multi-scan
2θ range (compl.)	4.7–54.2° (99.4%)	4.4–56.0° (100%)	4.5–60.0° (99.9%)	4.5–68.0° (99.7%)	4.5–68.0° (99.7%)	4.4–68.0° (99.4%)	5.0–70.0° (100%)
Refl. Measured	195 947	144 260	29 889	275 463	65 840	18 989	456 256
Unique (<i>R</i> _{int})	20 759 (0.1095)	10 365 (0.0465)	29 889	18 533 (0.0426)	13 137 (0.0315)	18 989	24 974 (0.0315)
observed ^a	13 218	9040	11 7184	16 987	12 617	16 575	21 349
Param./restr.	1143/0	511/0	593/70	534/0	552/0	547/0	579/0
<i>R</i> ₁ (obs. rflns.) ^a	0.0393	0.089	0.0356	0.0195	0.0189	0.0290	0.0262
<i>wR</i> ₂ (all rflns.)	0.0838	0.0516	0.0500	0.0444	0.0385	0.0623	0.0562
Goof on <i>F</i> ²	1.039	1.234	0.786	1.120	1.095	1.004	1.045
max./min. ρ/(e Å ⁻³)	1.646/–0.947	1.009/–0.724	2.305/–0.982	1.877/–1.095	0.518/–1.035	1.814/–1.177	1.860/–0.953
CCDC no.	1881540	1881536	1881534	1881538	1881541	1881537	1881542

^a Obs. criterion: *I* > 2σ(*I*). ^b The crystal is non-merohedrally twinned and contains disordered solvent. ^c The crystal is a non-merohedrally three-component twin.

13.2 Hz, $J_{C-Pt} = 13$ Hz (satellites), CH_{PPh_3} , 136.6 (virt. t, $J_{C-P} = 3.5$ Hz, $J_{C-Pt} = 11$ Hz (satellites), C_{PPh_3}), 136.7–137.0 (m, C_{PPh_3}), 151.1 (d, $J_{C-P} = 2.9$ Hz, C_{cat}). $\delta^{31}P\{^1H\}$ (202 MHz, C_6D_6 , rt): 30.9 ($J_{P-Pt} = 1520$ Hz (satellites), P_{PPh_3}), 35.6 ($J_{P-Pt} = 1745$ Hz (satellites), P_{PPh_3}). $\delta^{11}B\{^1H\}$ (161 MHz, C_6D_6 , rt): 46 (br. s, $\Delta w_{1/2} = 2135$ Hz).

[Pt(PPh₃)₂(Bneop)₂] (3cc). [Pt(PPh₃)₂(C₂H₄)] (2) (50 mg, 67 μ mol, 1.0 eq.) and B₂neop₂ (1cc) (15.1 mg, 67 μ mol, 1.0 eq.) were mixed in toluene (5 mL). The pale-yellow solution was stirred at room temperature for 6 h whilst flask was evacuated for a few seconds every 30 min. The solvent was removed under reduced pressure to give an off-white solid. The residue was recrystallised from THF/*n*-pentane at $-40^\circ C$ to give analytically pure **3cc** (36 mg, 38 μ mol, 57%) as colourless microcrystalline solid. Single crystals suitable for X-ray diffraction analysis were obtained by vapour diffusion of *n*-pentane into a THF solution at room temperature. Mp $154^\circ C$ (decomposition). Found: C, 58.6; H, 5.5. Calc. for $C_{46}H_{50}B_2O_4P_2Pt$ (**3cc**): C, 58.4; H, 5.3. δ^1H (500 MHz, C_6D_6 , rt): 0.70 (12H, s, $(O(CH_2)_2)_2C(CH_3)_2$), 3.20 (8H, br. s, $J_{H-Pt} = 7$ Hz (satellites), $(O(CH_2)_2)_2C(CH_3)_2$), 6.88–6.95 (18H, m, CH_{PPh_3}), 7.64–7.72 (12H, m, 2- CH_{PPh_3}). $\delta^{13}C\{^1H\}$ (125 MHz, C_6D_6 , rt): 22.7 ($(O(CH_2)_2)_2C(CH_3)_2$), 31.8 ($(O(CH_2)_2)_2C(CH_3)_2$), 72.0 (d, $J_{C-Pt} = 45$ Hz (satellites) $(O(CH_2)_2)_2C(CH_3)_2$), 127.7–127.9 (m, 3- CH_{PPh_3}), 128.9 (s, 4- CH_{PPh_3}), 134.8–135.7 (m, 2- CH_{PPh_3}), 137.8 (d, $J_{C-P} = 39$ Hz, $J_{C-Pt} = 21$ Hz (satellites) 1- CH_{PPh_3}). $\delta^{31}P\{^1H\}$ (202 MHz, C_6D_6 , rt): 31.1 ($J_{P-Pt} = 1440$ Hz (satellites)). $\delta^{11}B\{^1H\}$ (161 MHz, C_6D_6 , rt): 45 (br. s, $\Delta w_{1/2} = 1500$ Hz).

[Pt(PPh₃)₂(Bmap)₂] (3hh). [Pt(PPh₃)₂(C₂H₄)] (2) (70 mg, 94 μ mol, 1.0 eq.) and B₂map₂ (1hh) (24.8 mg, 94 μ mol, 1.0 eq.) were mixed in toluene (4 mL). The red solution was stirred at room temperature for 3.5 h whilst flask was evacuated for a few seconds every 30 min. The solvent was removed under reduced pressure to give a brownish solid that was washed with *n*-pentane (2 \times 2 mL) and dried *in vacuo* (36 mg, 37 μ mol, 39%). Single crystals suitable for X-ray diffraction analysis were obtained by vapour diffusion of *n*-pentane into a THF solution at $-40^\circ C$. mp $140^\circ C$ (decomposition). Found: C, 60.7; H, 4.7; N, 3.1%. Calc. for $C_{50}H_{44}B_2N_2O_{2.5}P_2Pt$ (**3hh**): C, 61.1; H, 4.5; N, 2.9%. δ^1H (600 MHz, C_6D_6 , rt): 2.13 (6H, s, NCH_3), 6.37 (2H, d, $J = 7.6$ Hz, 3- CH_{map}), 6.71 (2H, t, $J = 7.6$ Hz, 5- CH_{map}), 6.80 (2H, t, $J = 7.6$ Hz, 4- CH_{map}), 7.05 (2H, d, $J = 7.6$ Hz, 6- CH_{map}), 6.81–6.87 (18H, m, CH_{PPh_3}), 7.54–7.64 (apparent br. t, 12H, $J = 7.5$ Hz, 2- CH_{PPh_3}). $\delta^{13}C\{^1H\}$ (150 MHz, C_6D_6 , rt): 30.3 (s, $J_{C-Pt} = 23.3$ Hz (satellites), NCH_3), 107.1 (3- CH_{map}), 110.3 (6- CH_{map}), 117.3 (5- CH_{map}), 120.0 (4- CH_{map}), 127.8 (br. s, CH_{PPh_3}), 129.2 (CH_{PPh_3}), 134.1–134.4 (m, CH_{PPh_3}), 136.2 (d, $J_{C-P} = 41$ Hz, C_{PPh_3}), 140.8 (2- CH_{map}), 153.9 (1- CH_{map}). $\delta^{31}P\{^1H\}$ (121 MHz, C_6D_6 , rt): 32.8 ($J_{P-Pt} = 1610$ Hz (satellites), P_{PPh_3}). $\delta^{11}B\{^1H\}$ (96 MHz, C_6D_6 , rt): 47 (br. s, $\Delta w_{1/2} = 1740$ Hz).

Pt catalysed bis-borylation of alkynes (general procedure). In a nitrogen filled glovebox the diborane(4) derivative (**1**) (1.0 eq.) and the alkyne (1.3 eq.) were mixed in dry toluene in a Schlenk tube. [Pt(PPh₃)₂(C₂H₄)] (2) (3 mol%) was added and the solution was, outside of the glove box, heated to $80^\circ C$. The progress of the reaction was monitored by GC/MS analysis of aliquots (0.05 mL). After complete consumption of the diborane(4) all volatiles were removed *in vacuo* and the residue extracted with *n*-pentane

and filtered over Celite. After evaporation of the solvent *in vacuo* the bisborylation product is obtained.

(dmabB)(Ph)C \equiv C(Ph)(Bpin). 1ad (55 mg, 202 μ mol), Ph-C \equiv C-Ph (47 mg, 264 μ mol), **2** (4.3 mg, 5.8 μ mol, 3 mol%), toluene (5 mL), reaction time 72 h, off-white solid (44 mg, 98 μ mol, 48%). Single crystals suitable for X-ray diffraction were obtained by cooling a hot *n*-hexane solution to $4^\circ C$. mp 198 – $200^\circ C$. Found: C, 74.3; H, 7.2; N, 5.95%. Calc. for $C_{28}H_{32}B_2N_2O_2$: C, 74.7; H, 7.2; N, 6.2%. δ^1H (300 MHz, C_6D_6 , rt): 0.76 (12H, s, $OC(CH_3)_2$), 3.20 (6H, s, NCH_3), 6.84–6.91 (1H, m, CH_{dmab}), 6.93–7.00 (5H, m, CH_{Ph}), 7.06–7.13 (2H, m, CH_{dmab}), 7.13–7.21 (4H, m, CH_{Ph}), 7.37–7.43 (2H, m, CH_{Ph}). $\delta^{13}C\{^1H\}$ (75 MHz, C_6D_6 , rt): 24.5 ($OC(CH_3)_2$), 29.7 (NCH_3), 83.3 ($OC(CH_3)_2$), 108.3 (CH_{dmab}), 119.2 (CH_{dmab}), 126.4 (CH_{Ph}), 126.5 (CH_{Ph}), 128.0 (CH_{Ph}), 128.2 (CH_{Ph}), 129.7 (CH_{Ph}), 130.2 (CH_{Ph}), 138.9 (CH_{dmab}), 142.2 (CH_{Ph}), 143.0 (CH_{Ph}), the quaternary boron bound carbon atoms were not detected. $\delta^{11}B\{^1H\}$ (96 MHz, C_6D_6 , rt): 29.5 (s, $\Delta w_{1/2} = 484$ Hz). m/z (EI^+ , 70 eV, GC/MS) 450 [M]⁺, 393, 367, 350, 246, 188, 179, 162, 145, 69.

(dmabB)(Me)C \equiv C(Ph)(Bpin) (mixture of isomers). 1ad (100 mg, 368 μ mol), Me-C \equiv C-Ph (56 mg, 482 μ mol), **2** (8.3 mg, 11.0 μ mol, 3 mol%), toluene (10 mL), reaction time 122 h, brownish oil (133 mg, 343 μ mol, 93%). (dmabB)(Me)C \equiv C(Ph)(Bpin) (major component), δ^1H (600 MHz, C_6D_6 , rt): 0.74 (12H, s, $OC(CH_3)_2$), 1.93 (3H, s, $=C(Bdmab)CH_3$), 3.16 (6H, s, NCH_3), 7.00–7.02 (2H, m, CH_{dmab}), 7.10–7.15 (1H, m, 4- CH_{Ph}), 7.18–7.21 (2H, m, CH_{dmab}), 7.28–7.32 (2H, m, 3- CH_{Ph}), 7.41–7.44 (2H, m, 2- CH_{Ph}). $\delta^{13}C\{^1H\}$ (150 MHz, C_6D_6 , rt): 20.7 ($=C(Bdmab)CH_3$), 24.5 ($OC(CH_3)_2$), 29.5 (NCH_3), 83.0 ($OC(CH_3)_2$), 108.1 (CH_{dmab}), 119.0 (CH_{dmab}), 126.2 (4- CH_{Ph}), 128.4 (3- CH_{Ph}), 129.4 (2- CH_{Ph}), 139.0 (CH_{dmab}), 142.3 (CH_{Ph}), 144 (br., $BC=CB$), 148 (br., $BC=CB$). m/z (EI^+ , 70 eV, GC/MS) 388 (35) [M]⁺, 331 (21), 305 (20), 288 (100), 245 (18), 188 (15), 162 (31), 145 (27), 117 (30), 69 (10). m/z (HR- EI^+ , 70 eV, GC/MS) 388.25114 [M]⁺, calc. for $C_{23}H_{30}B_2N_2O_2$: 388.24934 (1.80 mmu). (pinB)(Me)C \equiv C(Ph)(Bdmab) (minor component) δ^1H (600 MHz, C_6D_6 , rt): 1.13 (12H, s, $OC(CH_3)_2$), 2.21 (3H, s, $=C(Bdmab)CH_3$), 3.52 (6H, s, NCH_3), 6.94–6.97 (2H, m, CH_{dmab}), 7.14–7.17 (2H, m, CH_{dmab}), 7.44–7.49 (2H, m, 2- CH_{Ph}), not all signals could be unambiguously identified. $\delta^{13}C\{^1H\}$ (150 MHz, C_6D_6 , rt): 18.5 ($=C(Bpin)CH_3$), 25.3 ($OC(CH_3)_2$), 30.9 (NCH_3), 82.7 ($OC(CH_3)_2$), 108.1 (CH_{dmab}), 118.9 (CH_{dmab}), 129.3 (2- CH_{Ph}), not all signals could be unambiguously identified. m/z (EI^+ , 70 eV, GC/MS) 388 (80) [M]⁺, 331 (74), 305 (40), 288 (100), 245 (30), 188 (90), 162 (43), 145 (42), 117 (66), 69 (33). m/z (HR- EI^+ , 70 eV, GC/MS) 388.25046 [M]⁺, calc. for $C_{23}H_{30}B_2O_2$: 388.24934 (1.12 mmu). $\delta^{11}B\{^1H\}$ (96 MHz, C_6D_6 , rt): 29.8 (s, $\Delta w_{1/2} = 348$ Hz), isomers not resolved.

(pinB)(Me)C \equiv C(Ph)(Bcat) (mixture of isomers). 3ab (100 mg, 407 μ mol), Me-C \equiv C-Ph (61 mg, 529 μ mol), **2** (9.1 mg, 12 μ mol, 3 mol%), toluene (10 mL), reaction time 2 h, brownish oil (146 mg, 403 μ mol, 99%). (pinB)(Me)C \equiv C(Ph)(Bcat) (major component), δ^1H (500 MHz, C_6D_6 , rt): 0.95 (12H, s, $OC(CH_3)_2$), 2.06 (3H, s, $=C(Bcat)CH_3$), 6.81–6.84 (2H, m, CH_{cat}), 6.99–7.04 (1H, m, 4- CH_{Ph}), 7.06–7.10 (2H, m, CH_{cat}), 7.10–7.15 (2H, m, 3- CH_{Ph}), 7.33–7.38 (2H, m, 2- CH_{Ph}). $\delta^{13}C\{^1H\}$ (125 MHz, C_6D_6 , rt): 17.7 ($=C(Bpin)CH_3$), 24.6 ($OC(CH_3)_2$), 84.2 ($OC(CH_3)_2$), 112.5 (CH_{cat}), 122.5 (CH_{cat}), 127.0 (4- CH_{Ph}), 128.7 (3- CH_{Ph}), 128.8 (2-



CH_{Ph}), 140.6 (C_{Ph}), 142 (br., BC=CB), 147 (br., BC=CB). 149.2 (C_{cat}). *m/z* (EI⁺, 70 eV, GC/MS) 362 (3) [M]⁺, 305 (28), 262 (7), 220 (5), 158 (7), 143 (17), 128 (11), 115 (12), 84 (100), 69 (28). *m/z* (HR-EI⁺, 70 eV, GC/MS) 362.18433 [M]⁺, calc. for C₂₁H₂₄B₂O₄: 362.18607 (−1.74 mmu). (catB)(Me)C=C(Ph)(Bpin) (minor component) δ_H (500 MHz, C₆D₆, rt): 0.97 (12H, s, OC(CH₃)₂), 1.97 (3H, s, =C(Bcat)CH₃), 6.85–6.89 (2H, m, CH_{cat}), 7.04–7.10 (1H, m, 4-CH_{Ph}, overlapping), 7.11–7.15 (2H, m, CH_{cat}, overlapping), 7.19–7.24 (2H, m, 3-CH_{Ph}), 7.31–7.36 (2H, m, 2-CH_{Ph}, overlapping). δ_{13C{1H}} (125 MHz, C₆D₆, rt): 18.5 (=C(Bcat)CH₃), 24.6 (OC(CH₃)₂, overlapping), 84.1 (OC(CH₃)₂), 112.6 (CH_{cat}), 122.7 (CH_{cat}), 126.7 (4-CH_{Ph}), 128.3 (3-CH_{Ph}), 129.0 (2-CH_{Ph}), 141.0 (C_{Ph}), 142 (br., BC=CB), 147 (br., BC=CB). 149.1 (C_{cat}), not all signals could be unambiguously identified. *m/z* (EI⁺, 70 eV, GC/MS) 362 (5) [M]⁺, 305 (100), 291 (9), 262 (7), 220 (10), 158 (25), 143 (70), 128 (37), 115 (73), 105 (33), 84 (25), 69 (32). *m/z* (HR-EI⁺, 70 eV, GC/MS) 362.18847 [M]⁺, calc. for C₂₁H₂₄B₂O₄: 362.18607 (2.40 mmu). δ_{11B{1H}} (160 MHz, C₆D₆, rt): 31.7 (s, Δ*w*_{1/2} = 522 Hz), isomers not resolved.

(neopB)(Me)C=C(Ph)(Bpin) (mixture of isomers). 3ac (100 mg, 417 μmol), Me-C≡C-Ph (63 mg, 542 μmol), 2 (9.4 mg, 13 μmol, 3 mol%), toluene (10 mL), reaction time 2.5 h, brownish oil (146 mg, 410 μmol, 98%). (neopB)(Me)C=C(Ph)(Bpin) (major component), δ_H (500 MHz, C₆D₆, rt): 0.67 (6H, s, OCH₂C(CH₃)₂), 1.12 (12H, s, OC(CH₃)₂), 2.05 (3H, s, =C(Bneop)CH₃), 3.41 (4H, s, OCH₂C(CH₃)₂), 7.03–7.08 (1H, m, 4-CH_{Ph}), 7.19–7.25 (2H, m, 3-CH_{Ph}), 7.39–7.42 (2H, m, 2-CH_{Ph}). δ_{13C{1H}} (125 MHz, C₆D₆, rt): 18.1 (=C(neop)CH₃), 21.9 (OCH₂-C(CH₃)₂), 25.1 (OC(CH₃)₂), 31.4 (OCH₂C(CH₃)₂), 72.0 (OCH₂-C(CH₃)₂), 83.1 (OC(CH₃)₂), 126.1 (4-CH_{Ph}), 128.3 (3-CH_{Ph}), 128.9 (2-CH_{Ph}), 143.0 (C_{Ph}), 146 (br., BC=CB), 151 (br., BC=CB). *m/z* (EI⁺, 70 eV, GC/MS) 356 (0.3) [M]⁺, 341 (2) [M-Me]⁺, 298 (4), 283 (3), 240 (5), 213 (4), 187 (3), 169 (2), 155 (3), 143 (12), 129 (6), 116 (12), 105 (4), 84 (100), 69 (16). *m/z* (HR-EI⁺, 70 eV, GC/MS) 341.20789 [M-Me]⁺, calc. for C₁₉H₂₇B₂O₄: 341.20954 (−1.66 mmu). (pinB)(Me)C=C(Ph)(Bneop) (minor component), δ_H (500 MHz, C₆D₆, rt): 0.64 (6H, s, OCH₂C(CH₃)₂), 1.16 (12H, s,

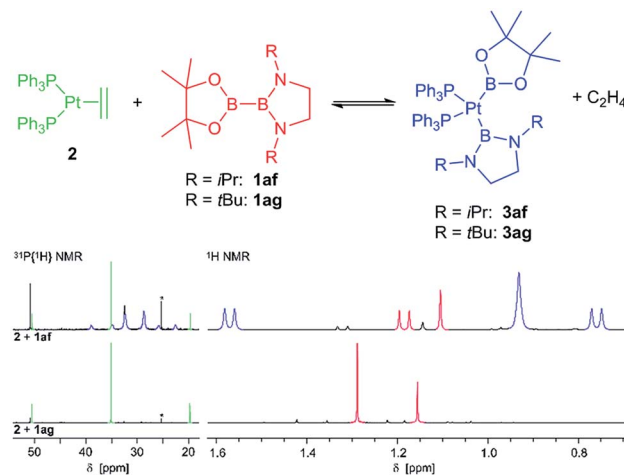


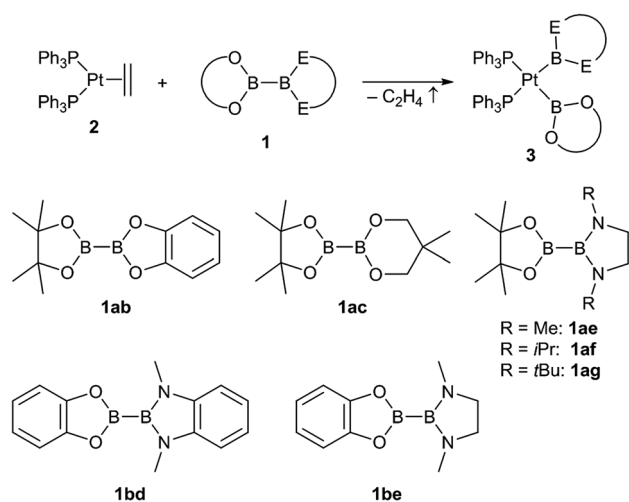
Fig. 1 NMR spectra of the reactions of 2 with 1af and 1ag, respectively. Top: 1af + 2, material obtained after eight cycles of evacuation (8 h). Bottom: *In situ* NMR spectra of 1ag + 2 after three cycles of evacuation (24 h). 300/122 MHz, rt, C₆D₆, *impurity of OPPh₃.

OC(CH₃)₂), 2.03 (3H, s, =C(Bneop)CH₃), 3.43 (4H, s, OCH₂-C(CH₃)₂), 7.03–7.08 (1H, m, 4-CH_{Ph}, overlapping), 7.19–7.25 (2H, m, 3-CH_{Ph}, overlapping), 7.39–7.42 (2H, m, 2-CH_{Ph}, overlapping). δ_{13C{1H}} (125 MHz, C₆D₆, rt): 18.1 (=C(Bneop)CH₃), 22.0 (OCH₂C(CH₃)₂), 25.1 (OC(CH₃)₂), 31.4 (OCH₂C(CH₃)₂), 72.2 (OCH₂C(CH₃)₂), 83.3 (OC(CH₃)₂), 126.1 (4-CH_{Ph}), 128.3 (3-CH_{Ph}), 128.9 (2-CH_{Ph}), 143.0 (C_{Ph}). (EI⁺, 70 eV, GC/MS) 356 (1) [M]⁺, 341 (5) [M-Me]⁺, 143 (13), 129 (8), 116 (100), 105 (8), 69 (42). *m/z* (HR-EI⁺, 70 eV, GC/MS) 356.23438 [M]⁺, calc. for C₂₀H₃₀B₂O₂: 356.23302 (1.37 mmu). δ_{11B{1H}} (96 MHz, C₆D₆, rt): 27.6 (s, Δ*w*_{1/2} = 417 Hz), 31.4 (s, Δ*w*_{1/2} = 424 Hz), isomers not resolved.

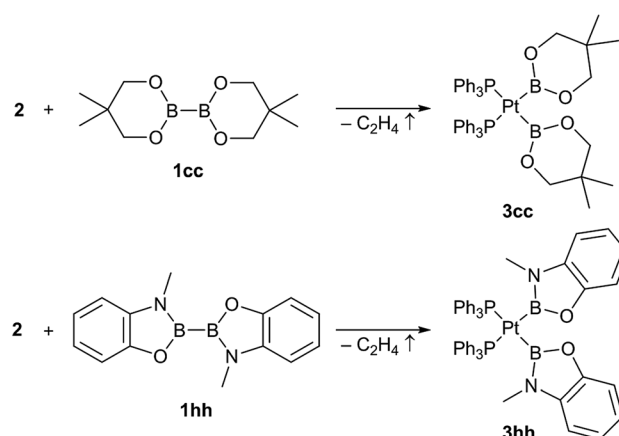
Results and discussion

Synthesis

The unsymmetrical platinum bis-boryl complexes 3ab, 3ac, 3ae, 3bd and 3be were obtained by oxidative addition of the respective unsymmetrical diborane(4) derivatives 1 to the platinum(0) complex 2 (Scheme 2). The procedure involved



Scheme 2 Synthesis of the unsymmetrical complexes (Ph₃P)₂-Pt(boryl)₂ 3ab, 3ac, 3ae, 3bd and 3be by oxidative addition of the respective unsymmetrical diboranes(4) 1 to [(Ph₃P)₂Pt(C₂H₄)] (2).



Scheme 3 Synthesis of the symmetrical bis-boryl platinum complexes (Ph₃P)₂Pt(boryl)₂ 3cc and 3hh.



repeated evacuation of the reaction mixture consisting of equimolar amounts of **1** and **2** in order to remove the formed ethene and shift the equilibrium of the reversible oxidative addition reaction to the product side.³ The unsymmetrical diboranes **1** employed comprise dialkoxy/aryloxy substituents such as Bpin (pin = (OCMe₂)₂), Bneop (neop = (OCH₂)₂CMe₂), Beat (cat = 1,2-O₂C₆H₄) as well as diamino substituents such as BMeEn (MeEn = (NMe)₂C₂H₄), Bdmab (dmab = 1,2-(NMe)₂C₆H₄) but also the sterically more demanding congeners BiPrEn (iPrEn = (NiPr)₂C₂H₄) and BtBuEn (tBuEn = (NtBu)₂-C₂H₄) (Scheme 2).

For the five unsymmetrical diboranes(**4**) **1ab**, **1ac**, **1ae**, **1bd** and **1be** the respective unsymmetrical platinum(II) complexes **3ab** (58%), **3ac** (52%), **3ae** (68%), **3bd** (58%) and **3be** (67%) were obtained as colourless or pale solids in good yields.

In contrast, with the sterically more demanding congeners of **1ae**, pinB-BiPrEn (**1af**) and pinB-BtBuEn (**1ag**), no platinum(II) complexes could be isolated. However, for the reaction of **1af** with **2** *in situ* NMR spectroscopy indicates that an oxidative addition to the complex [(Ph₃P)₂Pt(Bpin)(BiPrEn)] (**3af**) takes place (Fig. 1). According to ¹H NMR signals ratios a **1af** : **3af** ratio of 26 : 100 is obtained after repeated evacuation cycles. The ³¹P{¹H} NMR spectrum indicates also incomplete reaction, as besides the signals assigned to the complex **3af** unreacted **2** is observed (Fig. 1).⁹ In our hands all attempts to isolate **3af** resulted in mixtures of **1af**, **3af** and variable amounts of unidentified decomposition products (Fig. 1).⁹

With the more demanding **1ag**, however, no reaction is observed by *in situ* NMR spectroscopy (Fig. 1), as also reported for the related sterically demanding unsymmetrical diborane(**4**) pinB-Bdtab (tab = 1,2-(N(SiMe₃))₂C₆H₄).^{3,9}

In addition to those unsymmetrical complexes the symmetrical complexes [(Ph₃P)₂Pt(Bneop)₂] (**3cc**) and [(Ph₃P)₂-Pt(Bmap)₂] (**3hh**, map = 1,2-(O)(NMe)C₆H₄, derived from *N*-methylaminophenol)⁹ were analogously obtained from the respective symmetrical diborane(**4**) derivatives B₂neop₂ (**1cc**) and B₂map₂ (**1hh**) in yields of 57% and 39%, respectively (Scheme 3).

Crystallography

All five isolated unsymmetrical platinum(II) bis-boryl complexes **3ab**, **3ac**, **3ae**, **3bd** and **3be** as well as the two symmetrical complexes **3cc** and **3hh** were structurally characterized by single-crystal X-ray diffraction (Table 1). Well-developed single-crystals suitable for X-ray diffraction studies were typically obtained by vapour diffusion of *n*-pentane at room temperature into solutions of the complexes in benzene or THF typically within 16–30 h. This technique gave repeatedly well-developed, relatively large crystals, whilst crystallisation from the same or related solvents combinations (toluene instead of benzene) at –40 °C results frequently microcrystalline powders or intergrown crystals. However, as the platinum(II) bis-boryl complexes appear not indefinitely stable in solutions at room temperature (*vide infra*) comparably fast crystallization at room temperature appears favourable. The complexes **3ab**, **3ae**, **3be**, **3cc** and **3hh** crystallize as the solvates **3ab**(C₆H₆), **3ae**(C₄H₈O)_{1.5}, **3be**(C₆H₆),

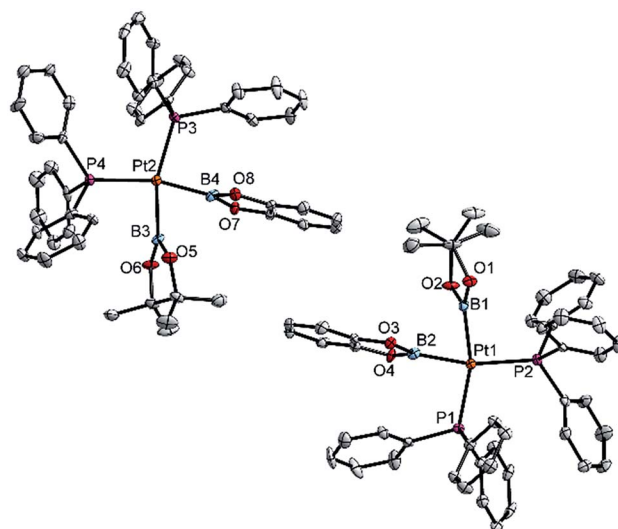


Fig. 2 Molecular structures of the two independent molecules of **3ab** in the crystal structure of **3ab**(C₆H₆) (Table 3). Selected distances (Å) and angles [°]: Pt1–P1 2.340(1), Pt1–P2 2.344(1), Pt1–B1 2.074(6), Pt1–B2 2.041(6), P1–Pt1–P2 104.97(5), B1–Pt1–B2 72.8(2), B1–Pt1–P2 92.9(2), B2–Pt1–P1 89.6(2), Σ(Pt1) 360.3(2); Pt2–P3 2.340(1), Pt2–P4 2.349(1), Pt2–B3 2.079(6), Pt2–B4 2.042(6), P3–Pt2–P4 105.55(5), B3–Pt2–B4 73.2(2), B3–Pt1–P4 92.1(2), B4–Pt2–P3 89.2(2), Σ(Pt1) 360.1(2).

3cc(C₄H₈O) and **3hh**(C₄H₈O) whereas **3ac** and **3bd** crystallize without co-crystallization of solvent. **3ab**(C₆H₆), **3bd**, **3be**(C₆H₆) and **3cc**(C₄H₈O) crystallize in the triclinic system in the space group type *P* $\bar{1}$, whilst **3ae**(C₄H₈O)_{1.5} and **3hh**(C₄H₈O) were found to crystallise in the monoclinic system (*P*₂₁/*c*), whereas **3ac** crystallises in the orthorhombic system (*Pbca*). Common to the solid state structures of all seven complexes is the absence of any molecular symmetry; all complexes are situated on general positions. For the complexes **3ac**, **3ae**, **3bd**, **3be**, **3cc** and **3hh** the asymmetric unit of the respective structures contain one independent complex molecule (*Z'* = 1), whereas for **3ab**(C₆H₆) two independent molecules of **3ab** as well as C₆H₆ are found in the asymmetric unit (*Z'* = 2). Contrary to the platinum complexes

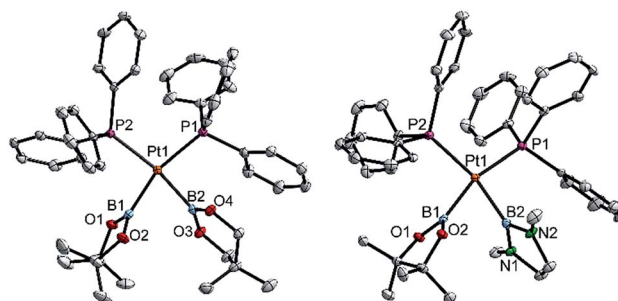


Fig. 3 Molecular structures of **3ac** (left) and **3ae** (right, from the crystal structure of **3ae**(C₄H₈O)_{1.5}, Table 3). Selected distances (Å) and angles [°]: **3ac**: Pt1–P1 2.3305(7), Pt1–P2 2.3376(7), Pt1–B1 2.071(3), Pt1–B2 2.084(3), P1–Pt1–P2 103.94(2), B1–Pt1–B2 75.1(1), B1–Pt1–P2 94.48(9), B2–Pt1–P1 88.19(9), Σ(Pt1) 361.7(1). **3ae**: Pt1–P1 2.3259(8), Pt1–P2 2.3325(8), Pt1–B1 2.062(4), Pt1–B2 2.088(4), P1–Pt1–P2 103.50(3), B1–Pt1–B2 71.9(1), B1–Pt1–P2 93.8(1), B2–Pt1–P1 90.8(1), Σ(Pt1) 360.0(1).



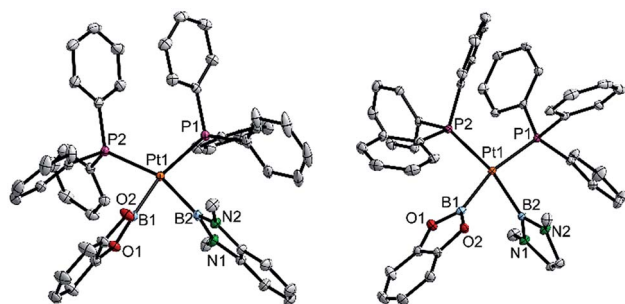


Fig. 4 Molecular structures of **3bd** (left) and **3be** (right, from the crystal structure of **3be**(C₆H₆), Table 3). Selected distances (Å) and angles [°]: **3bd**: Pt1–P1 2.3353(3), Pt1–P2 2.3462(3), Pt1–B1 2.041(2), Pt1–B2 2.089(2), P1–Pt1–P2 107.51(1), B1–Pt1–B2 75.55(6), B1–Pt1–P2 89.28(4), B2–Pt1–P1 92.11(4), $\Sigma(\text{Pt1})$ 364.5(1). **3be**: Pt1–P1 2.3328(4), Pt1–P2 2.3547(4), Pt1–B1 2.057(2), Pt1–B2 2.093(2), P1–Pt1–P2 102.98(1), B1–Pt1–B2 73.51(7), B1–Pt1–P2 92.39(5), B2–Pt1–P1 91.15(5), $\Sigma(\text{Pt1})$ 360.0(1).

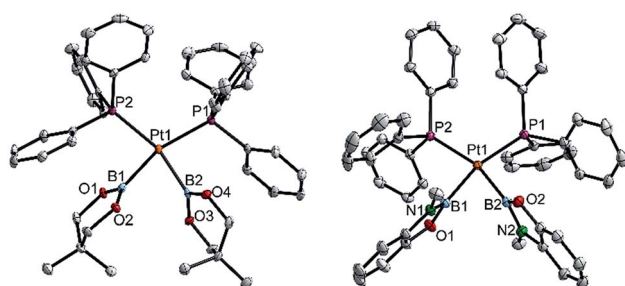


Fig. 5 Molecular structures of **3cc** (left, from the crystal structure of **3cc**(C₄H₈O)) and **3hh** (right, from the crystal structure of **3hh**(C₄H₈O), Table 3). Selected distances (Å) and angles [°]: **3cc**: Pt1–P1 2.348(1), Pt1–P2 2.345(1), Pt1–B1 2.085(5), Pt1–B2 2.075(4), P1–Pt1–P2 111.44(3), B1–Pt1–B2 76.18(13), B1–Pt1–P2 86.52(12), B2–Pt1–P1 86.99(12), $\Sigma(\text{Pt1})$ 361.1(5). **3hh**: Pt1–P1 2.3369(3), Pt1–P2 2.3409(3), Pt1–B1 2.073(1), Pt1–B2 2.065(2), P1–Pt1–P2 106.53(1), B1–Pt1–B2 73.80(6), B1–Pt1–P2 87.39(4), B2–Pt1–P1 92.27(4), $\Sigma(\text{Pt1})$ 360.0(1).

the solvent in **3ae**(C₄H₈O)_{1.5} and **3be**(C₆H₆) exhibits addition symmetry and resides (partially) on centres of inversion. In **3ae**(C₄H₈O)_{1.5} two distinct THF moieties are found, one on a centre of inversion and one on a general position, whereas in

3be(C₆H₆) the two independent molecules of benzene are located on the two distinct types of centres of inversion in *P*1̄. None of the structures exhibits disorder within the platinum bis-boryl complex, however, positional disorder is observed for one of the co-crystallized solvent molecules in **3ae**(C₄H₈O)_{1.5}.

All described platinum(II) bis-boryl complexes exhibit, as to be expected, a slightly distorted square-planar coordination environments at the platinum(II) (d⁸) ion with *cis*-arrangement of the boryl ligands. The sum of angles in the coordination sphere lies in a very narrow range of 360–362°, except for **3bd** where a value of 364.5(1)° is found (Fig. 2–5). The distortion from planarity towards a tetrahedron is, as indicated by the angle $\tau_{(\text{B},\text{B}/\text{P},\text{P})}$ included by the [B,Pt,B] and [P,Pt,P] planes, small but significant (Table 2).

All P–Pt distances are in a quite narrow range of 2.326–2.355 Å. These comparably long P–Pt distances are evidence for the generally strong *trans*-influence of boryl ligands, e.g. [(Ph₃P)₂PtCl₂] 2.26 Å, [(Ph₃P)₂Pt(*n*Bu)₂] 2.30 Å, [(Ph₃P)₂Pt(SiR₂H)₂] (R = Me, Ph) 2.34–2.37 Å.⁵

It has been proposed that the P–Pt distances are a suitable measure for the donor properties of a ligand in a complex [(Ph₃P)₂PtXY] (X, Y: anionic ligand), following the reasoning that a shortening of a *trans*-boryl P–Pt bond in dependence of a particular ligand indicates a relatively lower *trans*-influence of this ligand compared to a reference ligand, and analogously for the *cis*-influence of this ligand.⁷ However, the differences in P–Pt distances between the individual boryl ligands are quite small and appear not especially indicative for a comparison of the *trans*- and *cis*-influences of the individual boryl ligands given in Table 2. If at all, it may be stated that, taking **3aa** as a reference compound, all other boryl ligands have a relatively lower *trans*- and *cis*-influence.⁷ However, this contradicts experimental and computational studies suggesting a significantly stronger *trans*-influence of diamino boryl than dialkoxy boryl ligands.¹²

The Pt–B distances vary significantly and apparently systematically with the type of the individual boryl ligand (Table 2). Within the set of structures discussed here (Table 2) three types of boryl ligands may be defined: (i) (alkylO)₂B, such as Bpin and Bneop, (ii) aryloxyboryl ligands, here Bcat, (iii) and diamino boryl ligands, such as Bdmab and BMeEn. The first class

Table 2 Selected geometrical parameters of the complexes **3ab**, **3ac**, **3ad**,³ **3ae**, **3bd**, **3be**, **3aa**,^{4a} **3bb**,^{4c,13} **3cc** and **3hh**

3yz ¹⁷	B...B [Å]	$\tau_{(\text{B},\text{B}/\text{P},\text{P})}$ ^a [°]	P(y)–Pt [Å]	P(z)–Pt [Å]	B(y)–Pt [Å]	B(z)–Pt [Å]
3aa ^b	2.54(1)	3.6(2)	2.351(2)	2.353(1)	2.076(8)	2.077(6)
3ab ^c	2.443(8)	6.3(2)	2.340(1)	2.344(1)	2.074(6)	2.041(6)
	2.457(8)	2.3(2)	2.340(1)	2.349(1)	2.079(6)	2.042(6)
3ac	2.532(5)	14.60(8)	2.3305(7)	2.3376(7)	2.071(3)	2.084(3)
3ad ^d	2.448(5)	13.09(9)	2.3398(7)	2.3322(7)	2.078(3)	2.067(3)
3ae	2.430(6)	6.5(1)	2.3259(8)	2.3325(8)	2.062(4)	2.088(4)
3bb ^e	2.554(9)	9.3(2)	2.354(1)	2.347(1)	2.040(5)	2.058(6)
	2.443(2)	13.21(6)	2.3353(3)	2.3462(3)	2.041(2)	2.089(2)
3be	2.484(2)	2.09(5)	2.3328(4)	2.3547(4)	2.057(2)	2.093(2)
3cc	2.566(8)	11.4(1)	2.348(1)	2.345(1)	2.085(5)	2.075(4)
3hh	2.485(2)	6.25(4)	2.3369(3)	2.3409(3)	2.073(1)	2.065(2)

^a Angle included by the planes [B,Pt,B] and [P,Pt,P]. ^b $\Sigma(\text{Pt1})$ 359.9(4). ^c Two independent molecules in the asymmetric unit. ^d $\Sigma(\text{Pt1})$ 361.3(2).

^e $\Sigma(\text{Pt1})$ 360.2(3).



of ligands exhibits comparably long Pt–B distances in a range of 2.062–2.085 Å (0.003–0.008 Å esd) with an arithmetic mean of 2.076 Å (Table 2). Although slightly shorter values were found for individual B–Pt distances in the (alkylO)₂B complexes [(Ph₃P)₂Pt(B(OCH(COOMe))₂)] and [(Ph₃P)₂Pt(B(OCH₂C(H)PhO)₂)] (<2.06 Å) this range appears typical for this class of ligands.^{4d} In contrast the aryloxy substituted Bcat ligand leads to significantly shorter B–Pt distances in a range of 2.040–2.058 Å (0.002–0.006 Å esd) (arithmetic mean 2.047 Å). This agrees also with the Pt–B distances found for the catechol derived boryl ligands in [(Ph₃P)₂Pt(B(O₂C₆Cl₄))₂] (2.03(2), 2.04(2) Å) and [(Ph₃P)₂Pt(B(O₂C₆H₃-4-*t*Bu))₂] (2.046(13), 2.047(10) Å).^{4c,e} Finally, diamino-boryl ligands result in B–Pt distances comparable to those in dialkoxy boryl complexes but on the long side of those in aryloxy boryl complexes, as evidenced by the complexes **3ad**,³ **3ae**, **3bd** and **3be** exhibiting B–Pt distances in a range of 2.067–2.093 Å (0.002–0.003 Å esd) with an arithmetic mean of 2.084 Å. The latter agrees also with the distances reported for [(Ph₃P)₂Pt((NBn)₂C₆H₄)]₂ (2.092(2), 2.080(2) Å).³

The B···B distances are for all bis-boryl platinum(II) complexes of the type (Ph₃P)₂Pt(boryl)₂, reported in this work (Table 2) or in the literature, much shorter, <2.62 Å, than the doubled van-der-Waals radius of boron (3.84 Å).^{3,4,14a} However, those B···B distances are still much longer than those in the parent diborane(4) derivatives (averaged 1.7 Å, double covalent radii 1.68 Å).^{3,8,14b,15} However, those B···B distances are also longer than those found in bis-boryl cobalt complexes (2.19–2.27 Å) and a bis-boryl iridium complex (2.22 Å) where the presence of a three-centre metal–boron–boron interaction is supported by DFT computations.^{6d,16} Nonetheless, the short B···B distances still suggest an residual B···B interaction and, hence, the non-independence of the two boryl ligands within this series of complexes (*vide infra*).

NMR spectroscopy

The ¹¹B{¹H} spectra of **3ac**, **3ae**, **3af** (*in situ* NMR data, *vide supra*), **3be**, **3cc** and **3hh** exhibit very broad signals (1200–2500 Hz FWHM) around 47 ppm in agreement with the chemical shifts reported for related complexes.^{3,4} However, for none

of the unsymmetrical complexes **3ac**, **3ae**, **3af** and **3be** (and also **3ad** and [(Ph₃P)₂Pt((NBn)₂C₆H₄)]₂ (45 ppm, 3200 Hz)) two discernible signals for the two individual boryl ligands were observed.³ For the complexes **3ab** and **3bd**, however, no ¹¹B{¹H} NMR signal could be detected, presumably due to the very broad line shape of the quadrupolar ¹¹B nucleus in a low-symmetry environment and overlapping of the signals of the two three coordinate boron nucleus in the unsymmetrical boryl complexes. The narrow range and the averaged nature of these signals render an assignment of individual chemical shifts to specific boryl ligands impossible.

All new complexes **3ab**, **3ac**, **3ae**, **3af**, **3bd**, **3be**, **3cc** and **3hh** were also characterised in solution by ¹H, ¹³C{¹H}, and ³¹P{¹H} NMR spectroscopy. Beyond this, the complexes **3ab**, **3ac** and **3ae** allowed a more detailed characterisation by ¹H–¹H NOESY and ¹H–³¹P HMBC NMR spectroscopy allowing the assignment of the ³¹P{¹H} NMR signals *trans* to a specific boryl ligand (Table 3).³ For the other new unsymmetrical complexes **3bd** and **3be** this was not unambiguously possible for a lack of indicative ¹H–¹H NOESY contacts,⁹ whilst **3af** was not isolated in pure form and was characterised only *in situ* in the reaction mixture by NMR spectroscopy (*vide supra*).

The ³¹P{¹H} NMR chemical shifts of the phosphorous atom *trans* to a particular boryl ligand shows no systematic trend and varies *e.g.* for Bpin in a range of 4 ppm around 33.5 ppm (Table 3). However, for the ¹J_{Pt–P} coupling constants a certain systematic is discernible. The ¹J_{Pt–P} coupling *trans* to a Bpin ligand varies in a range of 100 Hz between 1515 Hz and 1615 Hz (this includes also [(Ph₃P)₂Pt((NBn)₂C₆H₄)(Bpin)]: *J*_{Pt–P}(*trans*-Bpin) 1530 Hz, *J*_{Pt–P}(*trans*-B((NBn)₂C₆H₄)) 1590 Hz), whereas for the closely related dialkoxy boryl ligand Bneop lower values of 1440 Hz (**3cc**) and 1455 Hz (**3ac**) are observed.^{3,12} For the diaryloxy ligand Bcat larger values above 1600 Hz are found, however, the restricted data set and the not unambiguously assigned data for **3bd** and **3be** renders this assignment tentative. Moreover, it should be noted that for the symmetrical **3bb** two distinct *J*_{Pt–P} coupling constants are reported.^{4b,c} From the data available it is clear that the ¹J_{Pt–P} coupling constant is not a viable measure of the *trans*-influence of the *trans*-boryl

Table 3 NMR spectroscopic data of **3ab**, **3ac**, **3ad**,³ **3ae**, **3af**, **3bd**, **3be**, **3aa**,^{4a} **3bb**,^{4b,c} **3cc** and **3hh** (161 MHz (¹¹B{¹H})) and 202 MHz (³¹P{¹H})), rt in C₆D₆)

3yz ¹⁷	δ _B ^a [ppm]	δ _P (y) [ppm]	<i>J</i> _{Pt–P} (y) [Hz]	δ _P (z) [ppm]	<i>J</i> _{Pt–P} (z) [Hz]
3aa	46.0	27.8	1515		
3ab		35.5	1565	28.7	1690
3ac	51 (2500)	33.7	1585	27.5	1455
3ad	47.5 (1680) ^b	34.5 ^b	1590 ^b	31.8 ^b	1715 ^b
3ae	47 (1600)	36.1	1615	31.1	1590
3af	45 (1200) ^c	28.7/32.4 ^c	1495/1600 ^c		
3bb	47.0 (br) ^{4c}	30.2 (ref. 4b)/28.7 (ref. 4c)	1610 (ref. 4b)/1640 (ref. 4c)		
3bd		31.0/33.7 ^d	1650/1715 ^d		
3be	46 (2135)	30.9/35.6 ^d	1520/1745 ^d		
3cc	45 (1500)	31.1	1440		
3hh	47 (1740)	32.8	1610		

^a Δ*w*_{1/2} (FWHM) [Hz] in parentheses. ^b Measured at 96 MHz (¹¹B{¹H}) and 162 MHz (³¹P{¹H}). ^c Not isolated, *in situ* NMR data. Measured at 96 MHz (¹¹B{¹H}) and 122 MHz (³¹P{¹H}). ^d No assignment to individual ligands conducted.



ligand.^{7,18} It is clear, as suggested earlier, that the ligand in *cis* position has an appreciable influence on the *trans* $^1J_{\text{Pt-P}}$ coupling constants (*cis* influence).³

Stability and decomposition

It has been earlier reported for **3ad** and $[(\text{PCy}_3)_2\text{Pt}(\text{B}(\text{OMe})_2)_2]$ that bis-boryl platinum(II) complexes exist in solution in equilibrium with their reductive elimination products, the parent diborane(4) and a platinum(0) complex $[(\text{R}_3\text{P})_2\text{Pt}]$.^{3,6a} This appears to hold also for the complexes **3ac**, **3ae** and **3bd**, as in the ^1H NMR spectra of freshly prepared samples of these complexes signals indicative for the respective parent diborane(4) derivatives (Fig. S2a, S3b and S4a†) were observed in minute amounts (**3ac** : **1ac** 25 : 1, **3ae** : **1ae** 30 : 1, **3bd** : **1bd** 100 : 1).⁹ However, only for **3bd** unambiguous exchange signals were detected by ^1H - ^1H NOESY spectroscopy (Fig. S4a†).⁹ Nonetheless, it must be emphasised that these complexes are not indefinitely stable in solution at room temperature and one of the decomposition products is the parent diborane(4) derivative itself.

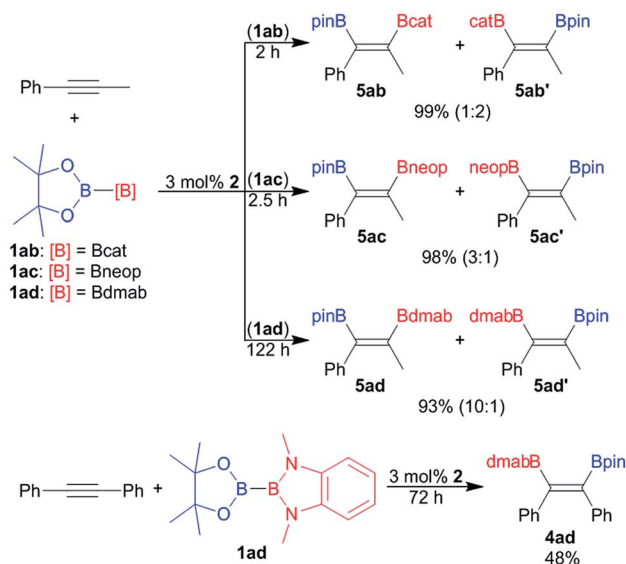
Freshly prepared C_6D_6 solutions of the bis-boryl platinum(II) complexes are virtually colourless but over time an intense reddish or orange colouration is observed.¹⁹ Exemplarily the decomposition of **3cc** was monitored by NMR spectroscopy over 38 h at ambient temperature in C_6D_6 and indicates the reductive elimination of the diborane(4), B_2neop_2 (**1cc**), along with the formation of so far unidentified platinum phosphine complexes (Fig. S7†).⁹

From solutions of the bis-boryl platinum(II) complexes **3** repeatedly intense orange crystals of $[(\text{Ph}_3\text{P})\text{Pt}(\mu\text{-PPh}_2)_2]$ and $[(\text{Ph}_3\text{P})_2\text{Pt}_3(\mu\text{-PPh}_2)_3\text{Ph}]$ (as their THF solvates) were obtained upon crystallisation at room temperatures after several days (*vide supra*) and were characterised crystallographically (Fig. S8 and S9†).⁹ These two complexes have been described previously as thermal decomposition products of **2**.²⁰

It should be noted that we could not observe any evidence for scrambling of the boryl ligands, hence the formation of symmetrical bis-boryl platinum complexes or symmetrical diborane(4) derivatives. Considering that this could proceed *e.g.* via a bimolecular ligand exchange between two unsymmetrical bis-boryl platinum(II) complexes, a reaction of a bis-boryl platinum(II) complexes and a free boryl ligand (*e.g.* from dissociation from a bis-boryl platinum(II) complexes) or *via* an oxidative addition/reductive elimination pathway of a bis-boryl platinum(II) complex and a diborane(4) derivative. All these reactions are apparently not favourable for the square-planar bis-boryl platinum(II) complexes considered here.

Catalysis

Since its introduction by Suzuki and co-worker in 1993 the platinum catalysed bis-borylation of alkynes with diborane(4) derivatives has been established as a facile and widely used access to 1,2-bis-borylated alkenes.² For these borylation reactions bis-boryl platinum complexes are established reactive intermediates.^{2,4a} More recently Sugimoto and co-worker have shown that the unsymmetrical diborane(4) pinB-Bdan (dan =



Scheme 4 Exemplary platinum catalysed bis-borylation of alkynes with unsymmetrical diboranes(4) **1ab**, **1ac** and **1ad**.

naphthalene-1,8-diaminato) may be used as reagent in the regioselective bis-borylation of unsymmetrical alkynes.²¹

The unsymmetrical diborane(4) derivatives **1ab**, **1ac** and **1ad** were exemplarily used to borylate the unsymmetrical alkyne $\text{Ph-C}\equiv\text{C-Me}$ (Scheme 4) in the presence of **2** as pre-catalyst. The bis-borylation proceeds smoothly with all three diboranes, yielding the respective unsymmetrically borylated alkenes **5** in excellent yields (Scheme 4). However, the dialkoxy diamino diboron reagent **1ad** reacts significantly slower than the unsymmetrical tetra alkoxy diboranes(4) **1ac** and **1ad** (Scheme 4). The sluggish reaction of **1ad** is also apparent in the bis-borylation of symmetrical diphenyl acetylene to give **4ad** (Scheme 4).

In the case of unsymmetrically substituted acetylene as substrates the bis-borylation gives mixtures of the regioisomers of the unsymmetrically bis-borylated alkenes (Scheme 4). The different regioisomeric bis-borylation products were assigned by ^1H - ^1H NOESY NMR spectroscopy and the isomeric ratio were determined on the basis of the ratio of the characteristic methyl group signals. The alkene **4ad** was also characterised by single crystal X-ray diffraction (Fig. S11†).⁹

The bis-borylation of $\text{Ph-C}\equiv\text{C-Me}$ proceeds for all diboranes **1ab**, **1ac** and **1ad** with some degree of selectivity (Scheme 4). For the dialkoxy diamino borane(4) **1ad** a selectivity of 1 : 10 in favour of the isomer **5ad** was observed, notably, the same preference, the Bpin moiety adjacent to the phenyl ring, was also reported for pinB-Bdan as borylating reagent.²¹ In contrast to that the selectivity with **1ab** and **1ac** is significantly lower, and for **1ab** even reversed. Hence, the isomer **5ab'** with the Bpin moiety located at the carbon atom remote from the phenyl ring becomes predominant. It may be speculated that the selectivity origins for steric reasons – the sterically less demanding boryl moiety favours the more encumbered position adjacent to the phenyl ring. However, more data are certainly needed to derive final conclusions.



Conclusions

The facile access to unsymmetrical diborane(4) derivatives enables for the first time the synthesis of a series of unsymmetrical platinum(II) bis-boryl complexes ($(\text{Ph}_3\text{P})_2\text{Pt}(\text{boryl})(\text{boryl}')$). The diborane(4) compounds used comprises seven combinations of dialkoxy boryl (Bpin, Bcat, Bneop) and diamino boryl (Bdmab, BMeEn, BiPrEn, BtBuEn) moieties. From these diborane(4) precursors five bis-boryl complexes ($(\text{Ph}_3\text{P})_2\text{Pt}(\text{boryl})(\text{boryl}')$) were obtained; the sterically demanding ligands BiPrEn and BtBuEn did not allow the isolation of the corresponding boryl complexes.

This series of complexes obtained was characterised spectroscopically as well as structurally. The most prominent feature of the distorted square-planar *cis*-bis-boryl platinum complexes is the short B...B distance of 2.44–2.55 Å, >1.2 Å shorter than the doubled van-der-Waals radius of boron. The *trans*-boryl P–Pt distances are comparably long but in a narrow range around 2.34 Å, as expected for the strongly *trans*-influencing boryl ligands. However, no distinct variations in the P–Pt distances within this series of boryl ligands is observed that allow to draw conclusions on the relative donor strength of the different boryl ligands. Similar is true for the ^{31}P – ^{195}Pt NMR coupling constants, that are indicative for the strongly donating/*trans*-influencing boryl ligands, but exhibit no systematic variations to allow conclusions on the coordination properties. These findings may be rationalised by the interaction of the two boryl ligands: whilst the complexes may well be described as platinum(II) bis-boryl complexes there is (residual) interaction between the two boryl ligands. In other words, the boryl ligands exhibit not only a significant *trans*-influence, but also a significant *cis*-influence. Hence, a specific pair of boryl ligands may be best considered as entity and not as two individual boryl ligands.

Conflicts of interest

There are no conflicts to declare.

Acknowledgements

C. K., W. D. and C. B. gratefully acknowledges support by a Research Grant (KL 2243/5-1) of the Deutsche Forschungsgemeinschaft (DFG) and by the Fonds der Chemischen Industrie. We acknowledge support by the German Research Foundation and the Open Access Publication Funds of the Technische Universität Braunschweig. The authors thank Ally-Chem Co. Ltd. for a generous gift of diborane(4) reagents.

Notes and references

- (a) For an overview on boryl complexes see: L. Dang, Z. Lin and T. B. Marder, *Chem. Commun.*, 2009, 3987–3995; (b) G. J. Irvine, M. J. G. Lesley, T. B. Marder, N. C. Norman, C. R. Rice, E. G. Robins, W. R. Roper, G. R. Whittell and L. J. Wright, *Chem. Rev.*, 1998, **98**, 2685–2722; (c) H. Braunschweig and M. Colling, *Coord. Chem. Rev.*, 2001, **223**, 1–51; (d) S. Aldridge and D. L. Coombs, *Coord. Chem. Rev.*, 2004, **248**, 535–559; (e) H. Braunschweig, R. D. Dewhurst and A. Schneider, *Chem. Rev.*, 2010, **110**, 3924–3957; (f) H. Braunschweig, *Angew. Chem., Int. Ed.*, 1998, **37**, 1786–1801.
- (a) For an overview on borylation catalysis see: R. Barbeyron, E. Benedetti, J. Cossy, J.-J. Vasseur, S. Arseniyadis and M. Smietana, *Tetrahedron*, 2014, **70**, 8431–8452; (b) T. Ishiyama and N. Miyaoura, *Chem. Rev.*, 2004, **3**, 271–280; (c) E. C. Neeve, S. J. Geier, I. A. I. Mkhalid, S. A. Westcott and T. B. Marder, *Chem. Rev.*, 2016, **116**, 9091–9161; (d) T. B. Marder and N. C. Norman, *Top. Catal.*, 1998, **5**, 63–73.
- C. Borner and C. Kleeberg, *Eur. J. Inorg. Chem.*, 2014, 2486–2489.
- (a) T. Ishiyama, N. Matsuda, M. Murata, F. Ozawa, A. Suzuki and N. Miyaoura, *Organometallics*, 1996, **15**, 713–720; (b) C. N. Iverson and M. R. Smith III, *J. Am. Chem. Soc.*, 1995, **117**, 4403–4404; (c) G. Lesley, P. Nguyen, N. J. Taylor, T. B. Marder, A. J. Scott, W. Clegg and N. C. Norman, *Organometallics*, 1996, **15**, 5137–5154; (d) W. Clegg, T. R. F. Johann, T. B. Marder, N. C. Norman, A. G. Orpen, T. M. Peakman, M. J. Quayle, C. R. Rice and A. J. Scott, *J. Chem. Soc., Dalton Trans.*, 1998, 1431–1438; (e) A. Kerr, T. B. Marder, N. C. Norman, A. G. Orpen, M. J. Quayle, C. R. Rice, P. L. Timms and G. R. Whittell, *Chem. Commun.*, 1998, 319–320; (f) D. Curtis, M. J. G. Lesley, N. C. Norman, A. G. Orpen and J. Starbuck, *J. Chem. Soc., Dalton Trans.*, 1999, 1687–1694; (g) W. Clegg, F. J. Lawlor, G. Lesley, T. B. Marder, N. C. Norman, A. G. Orpen, M. J. Quayle, C. R. Rice, A. J. Scott and F. E. S. Souza, *J. Organomet. Chem.*, 1998, **550**, 183–192.
- (a) H.-K. Fun, S. Chantapromma, Y.-C. Liu, Z.-F. Chen and H. Liang, *Acta Crystallogr., Sect. E: Struct. Rep. Online*, 2006, **E62**, m1252–m1254; (b) H. Arai, M. Takahashi, A. Noda, M. Nanjo and K. Mochida, *Organometallics*, 2008, **27**, 1929–1935; (c) M. S. Hannu-Kuure, A. Wagner, T. Bajorek, R. Oilunkaniemi, R. S. Laitinen and M. Ahlgren, *Main Group Chem.*, 2005, **4**, 49–68.
- (a) H. Braunschweig and A. Damme, *Chem. Commun.*, 2013, **49**, 5216–5218; (b) H. Braunschweig, P. Brenner, R. D. Dewhurst, F. Guethlein, J. O. C. Jimenez-Halla, K. Radacki, J. Wolf and L. Zöllner, *Chem.–Eur. J.*, 2012, **18**, 8605–8609; (c) H. Braunschweig, A. Damme and T. Kupfer, *Chem.–Eur. J.*, 2013, **19**, 14682–14686; (d) H. Schubert, W. Leis, H. A. Mayer and L. Wesemann, *Chem. Commun.*, 2014, **50**, 2738–2740; (e) H. Braunschweig, M. Lutz, K. Radacki, A. Schaumlöffel, F. Seeler and C. Unkelbach, *Organometallics*, 2006, **25**, 4433–4435; (f) H. Braunschweig, M. Kaupp, C. J. Adams, T. Kupfer, K. Radacki and S. Schinzel, *J. Am. Chem. Soc.*, 2008, **130**, 11376–11393; (g) S. Pospiech, M. Bolte, H.-W. Lerner and M. Wagner, *Organometallics*, 2014, **33**, 6967–6974; (h) H. Braunschweig, M. Lutz and K. Radacki, *Angew. Chem., Int. Ed.*, 2005, **44**, 5647–5651; (i) J. P. H. Charmant, C. Fan, N. C. Norman and P. G. Pringle, *Dalton Trans.*, 2007, 114–123; (j) H. Braunschweig, R. Bertermann, P. Brenner, M. Burzler, R. D. Dewhurst, K. Radacki and F. Seeler, *Chem.–Eur. J.*,



- 2011, **17**, 11828–11837; (k) H. Braunschweig, M. Fuss, S. K. Mohapatra, K. Kraft, T. Kupfer, M. Lang, K. Radacki, C. G. Daniliuc, P. G. Jones and M. Tamm, *Chem.–Eur. J.*, 2010, **16**, 11732–11743; (l) H. Braunschweig, T. Kupfer, M. Lutz, K. Radacki, F. Seeler and R. Sigritz, *Angew. Chem., Int. Ed.*, 2006, **45**, 8048–8051; (m) N. Lu, N. C. Norman, A. G. Orpen, M. J. Quayle, P. L. Timms and G. R. Whittell, *J. Chem. Soc., Dalton Trans.*, 2000, 4032–4037; (n) J. H. Muessig, D. Prieschl, A. Deißnerberger, R. D. Dewhurst, M. Dietz, J. O. C. Jiménez-Halla, A. Trumpp, S. R. Wang, C. Brunecker, A. Haefner, A. Gärtner, T. Thiess, J. Böhnke, K. Radacki, R. Bertermann, T. B. Marder and H. Braunschweig, *J. Am. Chem. Soc.*, 2018, **140**, 13056–13063.
- 7 L. Rigamonti, A. Forni, M. Manassero, C. Manassero and A. Pasini, *Inorg. Chem.*, 2010, **49**, 123–135.
- 8 W. Oschmann, C. Borner and C. Kleeberg, *Dalton Trans.*, 2018, **47**, 5318–5327.
- 9 See ESI for details.†
- 10 G. R. Fulmer, A. J. M. Miller, N. H. Sherden, H. E. Gottlieb, A. Nudelman, B. M. Stoltz, J. E. Bercaw and K. I. Goldberg, *Organometallics*, 2010, **29**, 2176–2179.
- 11 (a) D. Stalke, *Chem. Soc. Rev.*, 1998, **27**, 171–178; (b) *CrysAlisPro*, Version 1.171.36.28 – 1.171.40.21, Agilent Technologies, 2010–2012; (c) G. M. Sheldrick, *Acta Crystallogr.*, 2015, **A71**, 3–8; (d) G. M. Sheldrick, *Acta Crystallogr.*, 2015, **C71**, 3–8; (e) G. M. Sheldrick, *Acta Crystallogr.*, 2008, **A64**, 112–122; (f) L. J. Farrugia, *J. Appl. Crystallogr.*, 1999, **32**, 837–838; (g) A. L. Spek, *J. Appl. Crystallogr.*, 2003, **36**, 7–13; (h) D. Kratzert, J. J. Holstein and I. Krossing, *J. Appl. Crystallogr.*, 2015, **48**, 933–938; (i) C. F. Macrae, I. J. Bruno, J. A. Chisholm, P. R. Edgington, P. McCabe, E. Pidcock, L. Rodriguez-Monge, R. Taylor, J. van de Streek and P. A. Wood, *J. Appl. Crystallogr.*, 2008, **41**, 466–470; (j) *Diamond 4.2.2. – Crystal and Molecular Structure Visualization*, Crystal Impact, H. Putz and K. Brandenburg GbR, Bonn, Germany, 2016.
- 12 (a) J. Zhu, Z. Lin and T. B. Marder, *Inorg. Chem.*, 2005, **44**, 9384–9390; (b) H. Braunschweig, P. Brenner, A. Müller, K. Radacki, D. Rais and K. Uttinger, *Chem.–Eur. J.*, 2007, **13**, 7171–7176.
- 13 Data of (**3bb**(C₆D₆)) from ref. 4c; in ref. 4b another solvate (**3bb**(C₇H₈)) of **3bb** is reported. However, the latter data agree well with the one of **3bb**(C₆D₆), albeit with significant larger errors.
- 14 (a) M. Mantina, A. C. Chamberlin, R. Valero, C. J. Cramer and D. G. Truhlar, *J. Phys. Chem. A*, 2009, **113**, 5806–5812; (b) B. Cordero, V. Gómez, A. E. Platero-Prats, M. Revés, J. Echeverría, E. Cremades, F. Barragán and S. Alvarez, *Dalton Trans.*, 2008, 2832–2838.
- 15 M. Eck, S. Würtemberger-Pietsch, A. Eichhorn, J. H. J. Berthel, R. Bertermann, U. Paul, H. Schneider, A. Friedrich, C. Kleeberg, U. Radius and T. B. Marder, *Dalton Trans.*, 2017, **46**, 3661–3680.
- 16 (a) C. J. Adams, R. A. Baber, A. S. Batsanov, G. Bramham, J. P. H. Charmant, M. F. Haddow, J. A. K. Howard, W. H. Lam, Z. Lin, T. B. Marder, N. C. Norman and A. G. Orpen, *Dalton Trans.*, 2006, 1370–1373; (b) C. Dai, G. Stringer, J. F. Corrigan, N. J. Taylor, T. B. Marder and N. C. Norman, *J. Organomet. Chem.*, 1996, **513**, 273–275.
- 17 B(y) refers to properties of the boron atom in the boryl group y as given in the compound number **3yz**, referring to the naming scheme given in Schemes 2 and 3. Accordingly, P(y) refers to properties of the phosphorous atom *trans* to the boryl group y, this applies also to the NMR parameters $\delta P(y)$ and $J_{P-Pt}(y)$. An analogous naming scheme applies with respect to the boryl group z.
- 18 An attempt to differentiate between *trans* and *cis* influence implying an additive relation as suggested by Pasini and co-workers was not fruitful.⁷
- 19 It should be mentioned that even analytically pure samples of complexes **3** are often slightly coloured, presumably due to decomposition during preparation. However, a deepening of the reddish/orange colour of their solutions is clearly observed nonetheless.
- 20 (a) N. J. Taylor, P. C. Chieh and A. J. Carty, *J. Chem. Soc., Chem. Commun.*, 1975, 448–449; (b) W. Petz, C. Kutschera and B. Neumüller, *Organometallics*, 2005, **24**, 5038–5043; (c) R. Bender, P. Braunstein, A. Dedieu, P. D. Ellis, B. Huggins, P. D. Harvey, E. Sappa and A. Tiripicchio, *Inorg. Chem.*, 1996, **35**, 1223–1234; (d) R. Bender, P. Braunstein, A. Tiripicchio and M. Tiripicchio Camellini, *Angew. Chem., Int. Ed.*, 1985, **24**, 861–862.
- 21 N. Iwadate and M. Sugimoto, *J. Am. Chem. Soc.*, 2010, **132**, 2548–2549.

